

Environmental controls on silica sinter formation revealed by radiocarbon dating

Silvina Slagter^{1,2*}, Martin Reich^{1,2}, Carolina Munoz-Saez^{1,2}, John Southon³, Diego Morata^{1,2}, Fernando Barra^{1,2}, Jian Gong⁴, and J.R. Skok⁵

¹Department of Geology and Andean Geothermal Center of Excellence (CEGA), Facultad de Ciencias Físicas y Matemáticas, Universidad de Chile, Plaza Ercilla 803, Santiago, Chile

²Millennium Nucleus for Metal Tracing along Subduction, Facultad de Ciencias Físicas y Matemáticas, Universidad de Chile, Santiago, Chile

³Department of Earth System Science, University of California, Irvine, California 92697, USA

⁴Institut de Physique du Globe de Paris, CNRS-UMR7154, 75005 Paris, France

⁵SETI Institute, Mountain View, California 94043, USA

ABSTRACT

Silica sinter deposits overlying geothermal fields are reliable records of environmental, geochemical, and biological changes through time. Therefore, determining the absolute ages of formation of these deposits is fundamental to constrain the timing and evolution of processes that have shaped silica precipitation on the Earth's surface. We performed ¹⁴C dating of organic matter trapped within silica sinter deposits from the high-altitude El Tatio geyser field in the Chilean Altiplano. Radiocarbon ages of stratigraphically controlled samples retrieved from four well-preserved paleosinter mounds range from 10,840 ± 30 to 230 ± 35 yr B.P., indicating that the El Tatio system has had active discharge of silica-rich chloride springs over at least the past 10,000 years that has resulted in the formation of extensive sinter deposits. These ages are used to determine the silica precipitation rate at El Tatio, which was calculated to be between 0.14 and 2.57 kg/yr/m². These values are among the highest precipitation rates in geothermal systems for which data are available, and are consistent with *in situ* silica precipitation experiments at El Tatio (0.84–2.92 kg/yr/m²). Our results indicate that the extreme environmental conditions of the arid Chilean Altiplano, i.e., high evaporation and cooling rate of thermal waters and significant daily temperature oscillations, play a key role in the construction and preservation of silica sinter deposits.

INTRODUCTION

Silica sinter deposits are the surface expressions of underlying geothermal systems and form when near-neutral pH thermal waters discharge and cool at the surface, precipitating silica (Lynne et al., 2007, and references therein). They are found near hot springs, forming mounds, and are targets for exploration of concealed geothermal energy resources and epithermal Au-Ag deposits (Sillitoe, 2015). Sinter deposits have also been the focus of astrobiological investigations (Konhauser et al., 2003, and references therein), and recently the El Tatio geyser field in the central Andes has been proposed as an early-Mars analog environment because of similar siliceous sinter textures observed on the Martian surface (Ruff and Farmer, 2016). El Tatio is one of the

world's largest geyser fields and is located in the Chilean Altiplano at an altitude of 4200 m above sea level (a.s.l.), associated with extreme environmental conditions including high evaporation rates and daily air temperature oscillations that can reach up to 40 °C (Fig. 1). Silica sinter deposits at El Tatio cover an area of 30 km² with more than 200 thermal springs that host active sinters and fossil sinter, i.e., "paleosinter", deposits which are mostly concentrated in the upper basin (Fig. 1). This unique setting has motivated studies on the geochemistry and dynamics of thermal fluids, the mineralogy of sinter deposits, and the description of extremophile bacterial communities (Jones and Renaut, 1997; Fernandez-Turiel et al., 2005; Phoenix et al., 2006; Garcia-Valles et al., 2008; Nicolau et al., 2014; Munoz-Saez et al., 2016). Despite these advances, the absolute age of the El Tatio sinter deposits remains unconstrained, limiting

our knowledge about the evolution of the geothermal system at depth, the formation of sinter deposits on the surface, and the impacts of extreme environmental conditions on the rates of silica precipitation.

Determining the absolute age of silica sinter deposits is challenging. Previous studies have attempted to answer this question indirectly, either by relating hydrothermal deposits to glacial ages (White et al., 1988) or through estimations of the time that would be necessary to form the sinter deposits based on silica precipitation rates determined *in situ* (Nicolau et al., 2014). More recent geochronological studies, in contrast, have used radiocarbon dating techniques (¹⁴C) to obtain ages of organic carbon trapped within silica, opening new avenues for dating sinter deposits (Foley, 2006; Lynne et al., 2008; Lynne, 2012; Lowenstern et al., 2016).

In this study, we present 13 radiocarbon ages of stratigraphically controlled samples retrieved from four well-preserved paleosinter mounds at El Tatio. Our results point to a protracted history of silica precipitation with some of the oldest ¹⁴C ages reported so far for active geothermal fields. Our new radiocarbon ages are integrated with field observations and *in situ* experiments to determine the rates of silica precipitation at El Tatio, which point to a strong effect of environmental conditions on the construction of silica sinter deposits in high-altitude geothermal systems.

GEOLOGICAL BACKGROUND

El Tatio geyser field is bounded by a north-east-trending half-graben, which controls the orientation of most thermal manifestations (Fig. 1). The geyser field comprises extensive

*E-mail: sslagter@ing.uchile.cl

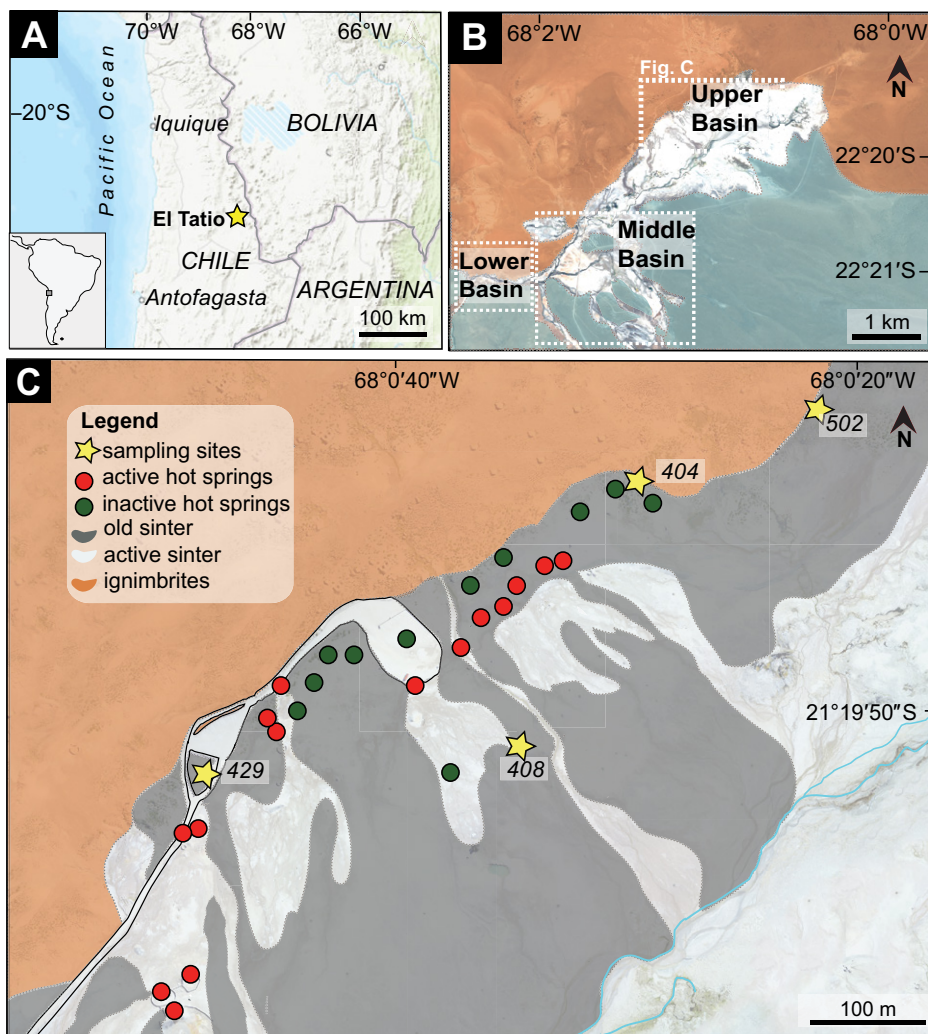


Figure 1. A: Location of El Tatio geysers in Chilean Altiplano. **B:** Map of El Tatio showing lower, middle, and upper basins in satellite image. White areas are silica sinter deposits; light green, glacial deposits; orange, ignimbrites. Modified from Munoz-Saez et al. (2018). **C:** Map of upper basin (white rectangle in B). Black lines are roads. Light blue lines are natural water courses. Mapping of surface thermal manifestations is overlain on drone image obtained in April 2017.

paleosinter deposits that precipitated over glacial sediments, and actively forming siliceous sinters with surface manifestations including thermal springs, fumaroles, geysers, and mud pools. Most of the hot springs discharge at temperatures close to the boiling point at 4200 m a.s.l. (~86 °C) and are characterized by near-neutral pH and high alkali chloride and silica concentrations (Cl >8000 mg/L, Na >3500 mg/L, and SiO₂ >150 mg/L) (Cusicanqui et al., 1975; Cortecci et al., 2005; Munoz-Saez et al., 2016).

The climate in this area is characterized by a low precipitation rate (<100 mm/yr). The mean annual temperature ranges from 8 to 11 °C during the day and day-night temperature variation often reaches 35°. In winter, the temperature can drop below -30 °C at night (Fernandez-Turiel et al., 2005). Wind direction is predominantly from the west with speeds between 3.7 and 7.5 m/s. The mean annual evaporation rate

at El Tatio is 131.9 mm/month, reaching its maximum during December (183.2 mm/month) and a minimum during June (72.8 mm/month) (Nicolau et al., 2014; Fig. DR7 in the GSA Data Repository¹).

These extreme environmental conditions have conditioned microbial life at El Tatio. Microbial communities that usually live in water temperatures close to 40 °C thrive under higher-temperature conditions (>60 °C) due to the high thermal gradient resulting from the strong Altiplano winds (Phoenix et al., 2006).

SAMPLES AND METHODS

We selected four well-preserved paleosinter mounds that represent former outflow zones in the upper basin (mounds 404, 502, 429, and 408;

¹GSA Data Repository item 2019113, textures, mineralogy, tables, and methods, is available online at <http://www.geosociety.org/datarepository/2019/>, or on request from editing@geosociety.org.

Fig. 1). We divided each mound from bottom to top into regular intervals (Fig. 2), and retrieved a 5-cm-thick sample at the base of each interval. The number of intervals in each mound depended on the height of the mound and the observed textures. The depositional environments and approximate temperature conditions can be inferred for each textural type by comparing the distinct textures preserved in the sampled paleosinter mounds with examples from modern geothermal settings (Lynne, 2012). The sampled mounds show textures that are characteristic of high-temperature conditions (60 °C) such as geysirite, as well as palisade and laminated textures that are similar to sinter textures described previously at El Tatio and which represent deposition at middle- to low-temperature conditions (40–20 °C) (Fig. DR1; Nicolau et al., 2014). Detailed examination using polarized light microscopy and scanning electron microscopy revealed that all of the sinter samples contain remnants of filamentous bacteria and plant fragments (Figs. DR2 and DR3). Bacteria are preserved within the siliceous matrix, which is predominantly opal-A (Fig. DR4). Details of the methods can be found in the Data Repository.

Two active geysers in the upper basin (sites 411 and 412) were selected for *in situ* silica precipitation experiments (see the Data Repository). At site 411, water is in equilibrium with amorphous silica, while at site 412, the geothermal water is undersaturated with respect to silica according to the equilibrium equation of Gunnarsson and Arnórsson (2000) (Table DR4 and Fig. DR6; see the Data Repository).

RADIOCARBON AGES

Radiocarbon and calibrated ages are reported in Table DR1. The ages of four paleosinter mounds comprise a time interval between 10,840 ± 30 yr B.P. and 230 ± 35 yr B.P. The oldest mound (mound 404) formed between 10,840 ± 30 and 5860 ± 25 yr B.P. and corresponds to a 1.5-m-tall structure with a smooth surface. Six intervals were sampled from this mound, with geysirite on top (sample 404a) and laminated and palisade textures at the bottom (samples 404f, 404e, 404d, 404c, and 404b) (Fig. 2A; Fig. DR1). Mound 408 has a height of 0.8 m, with a geysirite texture at the bottom (sample 408b; 7220 ± 45 yr B.P.) and a palisade texture at the top (sample 408t; 555 ± 20 yr B.P.). Mound 429 is 0.5 m high and has a gentle slope. Two layers are identified in this mound, with ages from 3720 ± 70 yr B.P. to 2625 ± 20 yr B.P. Lastly, mound 502 has a height of 2.4 m and was divided into three intervals. Radiocarbon dating yielded an age range of 2220 ± 15 yr B.P. to 230 ± 35 yr B.P. Laminated textures were found at the base (sample 502b), and geysirite and palisade textures were found in the middle (sample 502m) and top (sample 502t) layers, respectively (Fig. DR5). Most of the samples

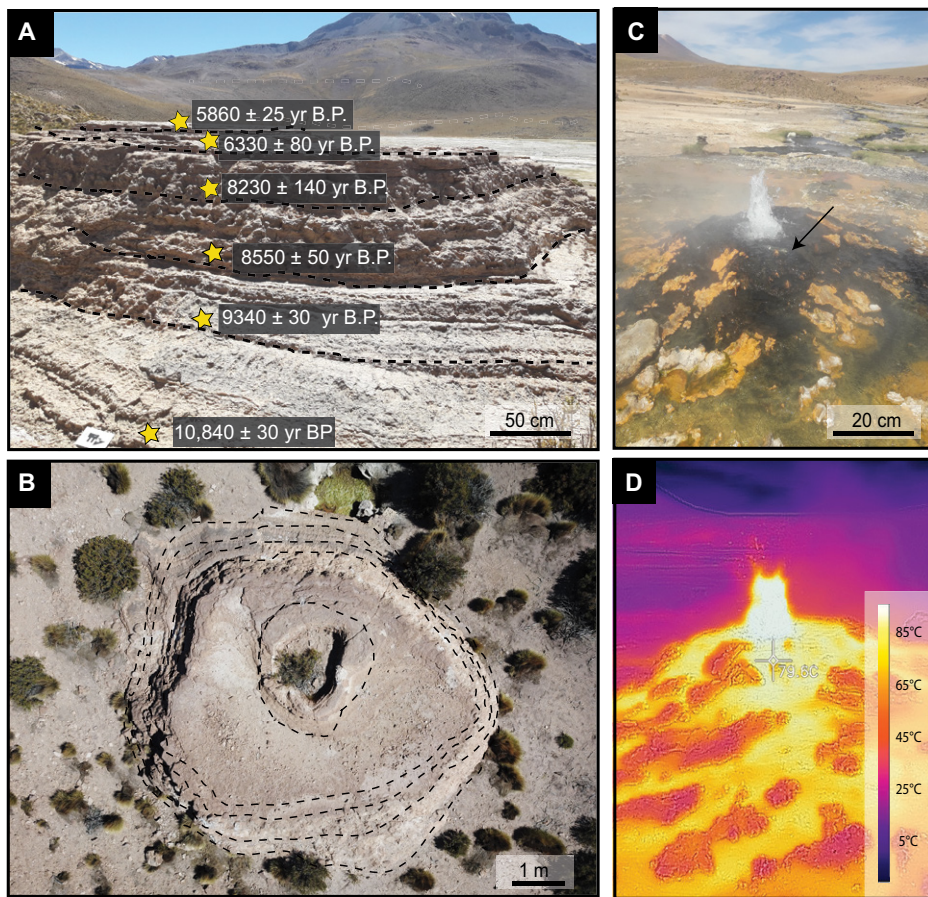


Figure 2. A: Paleosinter mound 404 with radiocarbon ages (in the El Tatio geyser field, Chilean Altiplano). Dashed lines represent limits of each interval. Yellow stars are sampling sites. **B:** Aerial drone image of mound 404 with dashed lines representing limits of each interval. For drone image details, see the Data Repository (see footnote 1). **C:** *In situ* precipitation experiment at active geyser site 411. Black arrow points to place where sandpaper sheets were placed. See the Data Repository for experimental methods. **D:** Thermal image of same geyser mound as in C, obtained with forward-looking infrared (FLIR) camera. Temperature of thermal water at experimental site was 78.8 °C.

consist of opal-A, which is present in samples younger than 8000 yr B.P. (Fig. DR4; see the Data Repository).

SILICA PRECIPITATION RATES

The silica precipitation rate for each layer within each mound was determined considering the thickness and extent of the layer (Table DR2). The thickness of each layer was measured directly from the mound, and the area was determined using aerial drone imaging (Fig. 2B; see the Data Repository). The precipitation rate R , in kg/yr/m^2 , was calculated using $R = \frac{A \cdot \rho}{\Delta t}$, where A is the layer thickness (m), ρ is density, assumed as 1.8 g/cm^3 based on previous density measurements in sinters (Herdianita et al., 2000; Munoz-Saez et al., 2016), and Δt is the difference in radiocarbon age between two consecutive layers. Silica precipitation rates were calculated considering a continuous precipitation process. In addition, the reported rates are considered minimum values because erosion was not taken into account.

Calculated silica precipitation rates for the four paleosinter mounds are between 0.14 and 2.57 kg/yr/m^2 (Figs. 3 and 4). It is worth noting that precipitation rates have varied at a given site through time. Mound 404 has varied from 0.1 to 0.9 kg/yr/m^2 , and in mound 502, precipitation has varied from 1.4 to 2.5 kg/yr/m^2 (Fig. 4). Foley (2006) suggested that pulses and pauses in silica sinter formation are due to variations in discharge rates and feature geometry changes. The higher precipitation rates observed in mound 502 may be due to either environmental changes or intrinsic variations in the hydrothermal system at depth.

The experimental precipitation rate varies between 0.84 and 2.92 kg/yr/m^2 (average 1.86 kg/yr/m^2 ; Table DR3), in agreement with previously reported *in situ* rates of 1.3 – 3.4 kg/yr/m^2 measured on glass slides (average 2.5 kg/yr/m^2 ; Nicolau et al., 2014). Silica precipitation rates determined for El Tatio are compared with published data for other geothermal systems (Fig. 3; see the Data Repository). In El Tatio, precipitation rates are among the highest measured in

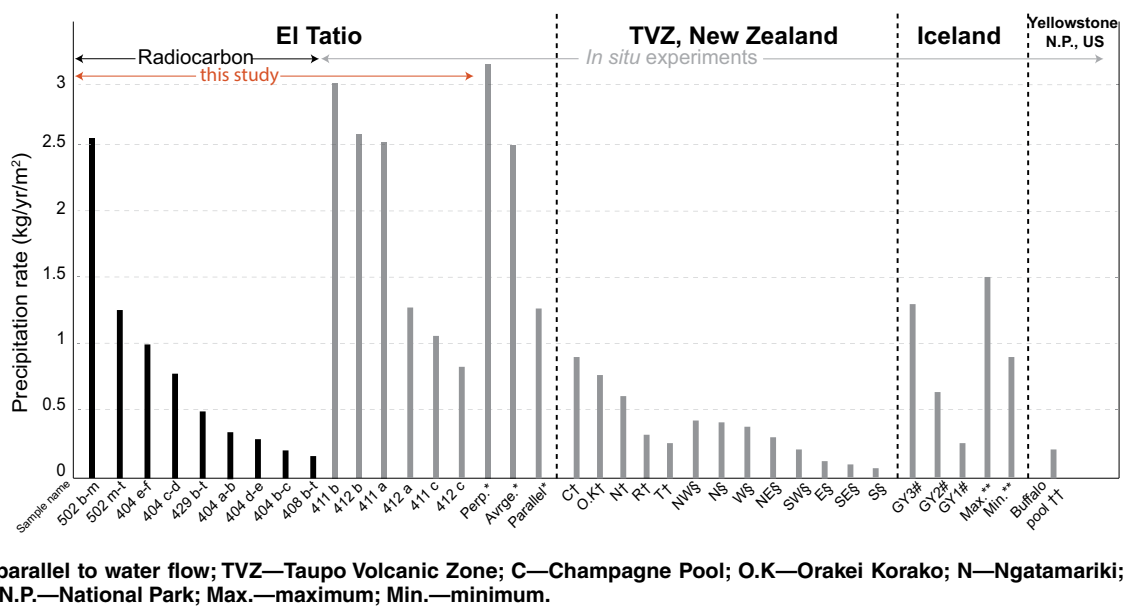
geothermal systems where data are available, reaching a maximum value of 3.4 kg/yr/m^2 (average of 2.5 kg/yr/m^2 ; Nicolau et al., 2014), corresponding to *in situ* measurements.

IMPACT OF EXTREME ENVIRONMENTAL CONDITIONS

The high silica precipitation rates measured at El Tatio raise some fundamental questions concerning the behavior of dissolved silica in thermal waters that discharge on the surface. It is well documented that silica precipitation in geothermal fields is strongly controlled by cooling, pH changes, silica concentration, and ionic strength (Hinman and Lindstrom, 1996; Guidry and Chafetz, 2003, and references therein; Tobler and Benning, 2013). However, when comparing El Tatio to other systems in New Zealand and Iceland, it is noted that factors such as pH, temperature, and silica saturation do not explain the observed differences in precipitation rates. For example, the pH of discharged waters in all localities is close to 7, except at Geysir, Iceland, where more alkaline values have been reported (pH ~ 8.5) (Tobler et al., 2008). Furthermore, the temperature of the thermal fluids is also similar, ranging from 70 to $96 \text{ }^\circ\text{C}$. Despite these similarities, the silica content of thermal waters is the lowest at El Tatio, with an average of $\sim 216 \text{ ppm SiO}_2$ (Nicolau et al., 2014; this study; Table DR4) compared with Champagne Pool (New Zealand, $\sim 430 \text{ ppm}$; Handley et al., 2005), Geysir (Iceland, $\sim 360 \text{ ppm}$; Tobler et al., 2008), and Yellowstone National Park (western United States, $\sim 750 \text{ ppm}$; Channing and Butler, 2007).

Environmental conditions have been reported to exert a critical influence on silica precipitation and texture development (Lynne, 2012; Nicolau et al., 2014; Campbell et al., 2015; Sanchez-Yanez et al., 2017; Lynne et al., 2019). Particularly, high evaporation and high cooling rates of thermal waters enhance silica precipitation (Hinman and Lindstrom, 1996). Complete evaporation has been shown to be seven to eight orders of magnitude more efficient than precipitation from a supersaturated solution (Boudreau and Lynne, 2012; Orange et al., 2013). At El Tatio, evaporation is intensified by the high altitude, high wind speed, and low atmospheric humidity (Nicolau et al., 2014; Fig. DR7). In addition, the cooling rate of thermal waters caused by the low air temperature is extreme, and drastic variability in temperature gradients along channels can reach $\sim 30 \text{ }^\circ\text{C}$ within a square decimeter (Dunckel et al., 2009). Furthermore, daily freezing and thawing cycles may also influence silica precipitation by causing formation of cryogenic opal-A (Fox-Powell et al., 2018). Previous studies at El Tatio have described microtextures (e.g., platelets, microcolumns, and ridges) resulting from freezing-thawing processes (Nicolau et al., 2014). Channing and Butler (2007) reported that

Figure 3. Comparison between silica precipitation rates at El Tatio (Chilean Altiplano) and those at other geothermal systems, estimated using radiocarbon data (black) and *in situ* precipitation experiments (gray). Suffixes correspond to intervals between two samples. *—Nicolau et al. (2014); †—Mountain et al. (2003); §—Handley et al. (2005); #—Tobler et al. (2008); **—Konhauser et al. (2001); ††—Braunstein and Lowe (2001). Compass directions correspond to names of samples in Handley et al. (2005). Perp.—perpendicular to water flow; Avrge.—average; Parallel—parallel to water flow; TVZ—Taupo Volcanic Zone; C—Champagne Pool; O.K—Orakei Korako; N—Ngatamariki; R—Rotokawa; T—Tokaanu; N.P.—National Park; Max.—maximum; Min.—minimum.



during freezing, particles become compressed by ice, physically forcing aggregate formation. The partial freezing of thermal waters also leads to an increase in the concentration of dissolved chemical components (such as Si, Na, and Cl) in the water, enhancing the silica precipitation rate (Fox-Powell et al., 2018).

CONCLUSIONS AND FURTHER IMPLICATIONS

Our new ages contribute to a better understanding of the geologic history of the El Tatio area, pointing to a long-lived geothermal system that has been active since at least 10,840 yr B.P. Hydrothermal activity at El Tatio may have begun after the last deglaciation (ca. 20–10 kyr B.P. in the Chilean Altiplano; Blard et al., 2014) and continued uninterrupted throughout the Holocene.

Our results show that silica precipitation rates at El Tatio estimated from *in situ* experiments are consistent with silica precipitation rates calculated based on radiocarbon data, and were most likely enhanced by environmental factors such as high evaporation rates and extreme temperature oscillations. Interestingly, our data show some significant secular variations in the silica precipitation rate at El Tatio. In particular, an increase of ~2 kg/yr/m² is observed within a 2.4-m-tall geyser mound in the past 2000 yr (Fig. 4). These variations may have been caused by fluctuations in the concentration of silica in the fluids due to changes in the geothermal system and/or environmental conditions.

Overall, the results presented here indicate that siliceous sinter deposits not only contain mineralogical and biogeochemical information that record the evolution of a geothermal

system, but are crucial for reconstructing the effects of climate change on silica precipitation, and potentially on the development of extremophiles on Earth, and possibly Mars.

ACKNOWLEDGMENTS

We thank science editor Judith Totman Parrish and three anonymous reviewers for their constructive and helpful comments. We also acknowledge Fondo de Financiamiento de Centros de Investigación en Áreas Prioritarias (FONDAP)—Comisión Nacional de Investigación Científica y Tecnológica (CONICYT) project 15090013 “Andean Geothermal Centre of Excellence (CEGA)” for providing financial support to carry out this research that included a Master of Science scholarship. Additional support was provided by the Iniciativa Milenio through Millennium Nucleus for Metal Tracing along Subduction grant NC130065. We also thank the communities of Caspana and Toconce in Chile for allowing us access to field sites at El Tatio. We thank Veronica Rodriguez for her help and support in the laboratory.

REFERENCES CITED

Blard, P.-H., Lavé, J., Farley, K.A., Ramirez, V., Jiménez, N., Martin, L.C.P., Charreau, J., Tibari, B., and Fornari, M., 2014, Progressive glacial retreat in the Southern Altiplano (Uturuncu volcano, 22°S) between 65 and 14 ka constrained by cosmogenic ³He dating: *Quaternary Research*, v. 82, p. 209–221, <https://doi.org/10.1016/j.yqres.2014.02.002>.

Boudreau, A.E., and Lynne, B.Y., 2012, The growth of siliceous sinter deposits around high-temperature eruptive hot springs: *Journal of Volcanology and Geothermal Research*, v. 247–248, p. 1–8, <https://doi.org/10.1016/j.jvolgeores.2012.07.008>.

Braunstein, D.G., and Lowe, D.R., 2001, Relationship between spring and geyser activity and the deposition and morphology of high temperature (73 °C) siliceous sinter, Yellowstone National Park, Wyoming, U.S.A: *Journal of Sedimentary Research*, v. 71, p. 747–763, <https://doi.org/10.1306/2DC40965-0E47-11D7-8643000102C1865D>.

Campbell, K.A., Guido, D.M., Gautret, P., Foucher, F., Ramboz, C., and Westall, F., 2015, Geysers in hot-spring siliceous sinter: Window on Earth’s hottest terrestrial (paleo)environment and

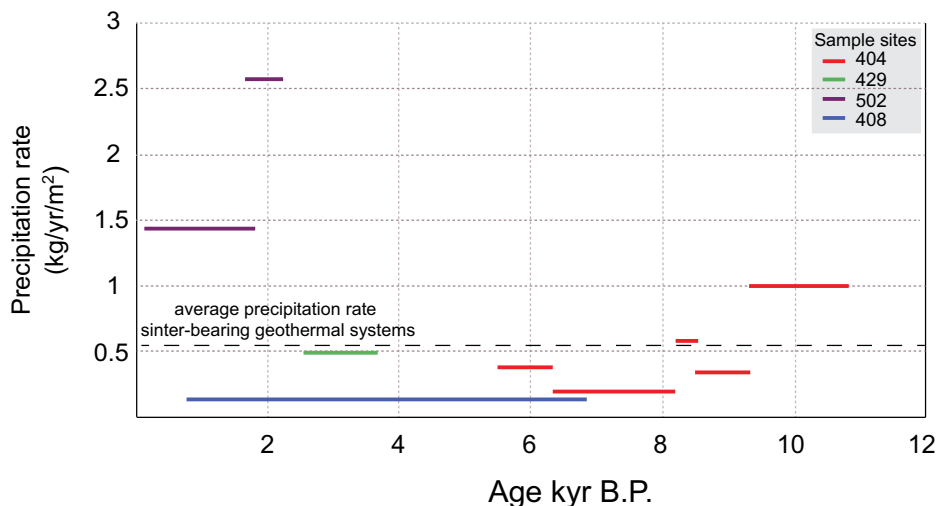


Figure 4. Silica precipitation rates at El Tatio (Chilean Altiplano) estimated using radiocarbon ages and plotted as function of time. Average rate corresponds to a global average, including data in Figure 3.

- its extreme life: *Earth-Science Reviews*, v. 148, p. 44–64, <https://doi.org/10.1016/j.earscirev.2015.05.009>.
- Channing, A., and Butler, I.B., 2007, Cryogenic opal-A deposition from Yellowstone hot springs: *Earth and Planetary Science Letters*, v. 257, p. 121–131, <https://doi.org/10.1016/j.epsl.2007.02.026>.
- Cortecci, G., Boschetti, T., Mussi, M., Herrera Lameli, C., Mucchino, C., and Barbieri, M., 2005, New chemical and original isotopic data on waters from El Tatio geothermal field, northern Chile: *Geochemical Journal*, v. 39, p. 547–571, <https://doi.org/10.2343/geochemj.39.547>.
- Cusicanqui, H., Mahon, W.A.J., and Ellis, A.J., 1975, The geochemistry of the El Tatio geothermal field, northern Chile, in *Proceedings of the Second United Nations Symposium on the Development and Use of Geothermal Resources*: Berkeley, California, Lawrence Berkeley Laboratory, p. 703–711.
- Dunckel, A.E., Cardenas, M.B., Sawyer, A.H., and Bennett, P.C., 2009, High-resolution in-situ thermal imaging of microbial mats at El Tatio Geyser, Chile shows coupling between community color and temperature: *Geophysical Research Letters*, v. 36, L23403, <https://doi.org/10.1029/2009GL041366>.
- Fernandez-Turiel, J.L., Garcia-Valles, M., Gimeno-Torrente, D., Saavedra-Alonso, J., and Martinez-Manent, S., 2005, The hot spring and geyser sinters of El Tatio, northern Chile: *Sedimentary Geology*, v. 180, p. 125–147, <https://doi.org/10.1016/j.sedgeo.2005.07.005>.
- Foley, D., 2006, Dating Castle Geyser: Preliminary results and broad speculations on the geologic development of geysers and hydrothermal systems in Yellowstone National Park, Wyoming, USA: *Geothermal Resources Council Transactions*, v. 30, p. 413–417.
- Fox-Powell, M.G., Channing, A., Applin, D., Cloutis, E., Preston, L.J., and Cousins, C.R., 2018, Cryogenic silicification of microorganisms in hydrothermal fluids: *Earth and Planetary Science Letters*, v. 498, p. 1–8, <https://doi.org/10.1016/j.epsl.2018.06.026>.
- Garcia-Valles, M., Fernandez-Turiel, J.L., Gimeno-Torrente, D., Saavedra-Alonso, J., and Martinez-Manent, S., 2008, Mineralogical characterization of silica sinters from the el Tatio geothermal field, Chile: *American Mineralogist*, v. 93, p. 1373–1383.
- Guidry, S.A., and Chafetz, H.S., 2003, Depositional facies and diagenetic alteration in a relict siliceous hot spring accumulation: Examples from Yellowstone National Park, U.S.A.: *Journal of Sedimentary Research*, v. 73, p. 806–823, <https://doi.org/10.1306/022803730806>.
- Gunnarsson, I., and Arnórsson, S., 2000, Amorphous silica solubility and the thermodynamics properties of H_4SiO_4 in the range of 0° to 350°C at P_{sat} : *Geochimica et Cosmochimica Acta*, v. 64, p. 2295–2307, [https://doi.org/10.1016/S0016-7037\(99\)00426-3](https://doi.org/10.1016/S0016-7037(99)00426-3).
- Handley, K.M., Campbell, K.A., Mountain, B.W., and Browne, P.R.L., 2005, Abiotic-biotic controls on the origin and development of spicular sinter: *In situ* growth experiments, Champagne Pool, Waitotapu, New Zealand: *Geobiology*, v. 3, p. 93–114, <https://doi.org/10.1111/j.1472-4669.2005.00046.x>.
- Herdianita, N.R., Browne, P.R.L., Rodgers, K.A., and Campbell, K.A., 2000, Mineralogical and textural changes accompanying ageing of silica sinter: *Mineralium Deposita*, v. 35, p. 48–62, <https://doi.org/10.1007/s001260050005>.
- Hinman, N.W., and Lindstrom, R.F., 1996, Seasonal changes in silica deposition in hot spring systems: *Chemical Geology*, v. 132, p. 237–246, [https://doi.org/10.1016/S0009-2541\(96\)00060-5](https://doi.org/10.1016/S0009-2541(96)00060-5).
- Jones, B., and Renaut, R.W., 1997, Formation of silica oncoids around geysers and hot springs at El Tatio, northern Chile: *Sedimentology*, v. 44, p. 287–304, <https://doi.org/10.1111/j.1365-3091.1997.tb01525.x>.
- Konhauser, K.O., Phoenix, V.R., Bottrell, S.H., Adams, D.G., and Head, I.M., 2001, Microbial-silica interactions in Icelandic hot spring sinter: Possible analogues for some Precambrian siliceous stromatolites: *Sedimentology*, v. 48, p. 415–433, <https://doi.org/10.1046/j.1365-3091.2001.00372.x>.
- Konhauser, K.O., Jones, B., Reysenbach, A., and Renaut, R.W., 2003, Hot spring sinters: Keys to understanding Earth's earliest life forms: *Canadian Journal of Earth Sciences*, v. 40, p. 1713–1724, <https://doi.org/10.1139/e03-059>.
- Lowenstern, J.B., Hurwitz, S., and McGeehin, J.P., 2016, Radiocarbon dating of silica sinter deposits in shallow drill cores from the Upper Geyser Basin, Yellowstone National Park: *Journal of Volcanology and Geothermal Research*, v. 310, p. 132–136, <https://doi.org/10.1016/j.jvolgeores.2015.12.005>.
- Lynne, B.Y., 2012, Mapping vent to distal-apron hot spring paleo-flow pathways using siliceous sinter architecture: *Geothermics*, v. 43, p. 3–24, <https://doi.org/10.1016/j.geothermics.2012.01.004>.
- Lynne, B.Y., Campbell, K.A., James, B.J., Browne, P.R.L., and Moore, J.N., 2007, Tracking crystallinity in siliceous hot-spring deposits: *American Journal of Science*, v. 307, p. 612–641, <https://doi.org/10.2475/03.2007.03>.
- Lynne, B.Y., Campbell, K.A., Moore, J.N., and Browne, P.R.L., 2008, Origin and evolution of the Steamboat Springs siliceous sinter deposit, Nevada, U.S.A.: *Sedimentary Geology*, v. 210, p. 111–131, <https://doi.org/10.1016/j.sedgeo.2008.07.006>.
- Lynne, B.Y., Boudreau, A., Smith, I.J., and Smith, G.J., 2019, Silica accumulation rates for siliceous sinter at Orakei Korako geothermal field, Taupo Volcanic Zone, New Zealand: *Geothermics*, v. 78, p. 50–61, <https://doi.org/10.1016/j.geothermics.2018.11.007>.
- Mountain, B.W., Benning, L.G., and Boerema, J.A., 2003, Experimental studies on New Zealand hot spring sinters: Rates of growth and textural development: *Canadian Journal of Earth Sciences*, v. 40, p. 1643–1667, <https://doi.org/10.1139/e03-068>.
- Munoz-Saez, C., Saltiel, S., Manga, M., Nguyen, C., and Gonnermann, H., 2016, Physical and hydraulic properties of modern sinter deposits: El Tatio, Atacama: *Journal of Volcanology and Geothermal Research*, v. 361, p. 156–168, <https://doi.org/10.1016/j.jvolgeores.2016.06.026>.
- Munoz-Saez, C., Manga, M., and Hurwitz, S., 2018, Hydrothermal discharge from the El Tatio basin, Atacama, Chile: *Journal of Volcanology and Geothermal Research*, v. 325, p. 25–35, <https://doi.org/10.1016/j.jvolgeores.2018.07.007>.
- Nicolau, C., Reich, M., and Lynne, B., 2014, Physico-chemical and environmental controls on siliceous sinter formation at the high-altitude El Tatio geothermal field, Chile: *Journal of Volcanology and Geothermal Research*, v. 282, p. 60–76, <https://doi.org/10.1016/j.jvolgeores.2014.06.012>.
- Orange, F., Lalonde, S.V., and Konhauser, K.O., 2013, Experimental simulation of evaporation-driven silica sinter formation and microbial silicification in hot spring systems: *Astrobiology*, v. 13, p. 163–176, <https://doi.org/10.1089/ast.2012.0887>.
- Phoenix, V.R., Bennett, P.C., Engel, A.S., Tyler, S.W., and Ferris, F.G., 2006, Chilean high-altitude hot spring sinters: A model system for UV screening mechanisms by early Precambrian cyanobacteria: *Geobiology*, v. 4, p. 15–28, <https://doi.org/10.1111/j.1472-4669.2006.00063.x>.
- Ruff, S.W., and Farmer, J.D., 2016, Silica deposits on Mars with features resembling hot spring biosignatures at El Tatio in Chile: *Nature Communications*, v. 7, 13554, <https://doi.org/10.1038/ncomms13554>.
- Sanchez-Yanez, C., Reich, M., Leisen, M., Morata, D., and Barra, F., 2017, Geochemistry of metals and metalloids in siliceous sinter deposits: Implications for elemental partitioning into silica phases: *Applied Geochemistry*, v. 80, p. 112–133, <https://doi.org/10.1016/j.apgeochem.2017.03.008>.
- Sillitoe, R.H., 2015, Epithermal paleosurfaces: *Mineralium Deposita*, v. 50, p. 767–793, <https://doi.org/10.1007/s00126-015-0614-z>.
- Tobler, D.J., and Benning, L.G., 2013, *In situ* and time resolved nucleation and growth of silica nanoparticles forming under simulated geothermal conditions: *Geochimica et Cosmochimica Acta*, v. 114, p. 156–168, <https://doi.org/10.1016/j.gca.2013.03.045>.
- Tobler, D.J., Stefánsson, A., and Benning, L.G., 2008, *In-situ* grown silica sinters in Icelandic geothermal areas: *Geobiology*, v. 6, p. 481–502, <https://doi.org/10.1111/j.1472-4669.2008.00179.x>.
- White, D.E., Hutchinson, R.A., and Keith, T.E.C., 1988, The geology and remarkable thermal activity of Norris Geyser Basin, Yellowstone National Park, Wyoming: *U.S. Geological Survey Professional Paper* 1456, 84 p.

Printed in USA